

A FRACTIONAL-ORDER TUMOR GROWTH INHIBITION MODEL IN PKPD

JONG HYUK BYUN AND IL HYO JUNG

ABSTRACT. Many compartment models assume a kinetically homogeneous amount of materials that have well-stirred compartments. However, based on observations from such processes, they have been heuristically fitted by exponential or gamma distributions even though biological media are inhomogeneous in real environments. Fractional differential equations using a specific kernel in Pharmacokinetic/Pharmacodynamic (PKPD) model are recently introduced to account for abnormal drug disposition. We discuss a tumor growth inhibition (TGI) model using fractional-order derivative from it. This represents a tumor growth delay by cytotoxic agents and additionally show variations in the equilibrium points by the change of fractional order. The result indicates that the equilibrium depends on the tumor size as well as a change of the fractional order. We find that the smaller the fractional order, the smaller the equilibrium value. However, a difference of them is the number of concavities and this indicates that TGI over time profile for fitting or prediction should be determined properly either fractional order or tumor sizes according to the number of concavities shown in experimental data.

Received December 16, 2019; Accepted January 20, 2020.

2010 *Mathematics Subject Classification.* 92C55, 26A33, 34K37 .

Key words and phrases. Pharmacokinetics and pharmacodynamics (PKPD), Fractional differential equation (FDE), Emax model, Anomalous kinetic, Fractional-order tumor growth inhibition (FTGI), Fractional calculus .

This work was financially supported by the National Research Foundation of Korea (NRF) grant funded by the Korea government (MSIT) (NRF-2019R1A2C2007249).

©2020 The Youngnam Mathematical Society
(pISSN 1226-6973, eISSN 2287-2833)

Introduction

A compartment model [1] is a system of ODEs that consists of a finite number of compartments, each of which is homogeneous and well mixed. The coupled terms in ODEs interact among themselves using constant rates. Unlike normal diffusion by Fick's law, over the past few decades, strong experimental evidence has indicated that there exists super-diffusion or sub-diffusion [2]. Moreover, anomalous kinetics can also result from reaction-limited processes and long-time trapping. It is considered that anomalous kinetics introduces memory effects to the process [1], yielding age-structured integrodifferential equations [3, 4].

Interest in the fractional-order derivative has also increased in the area of PKPD [5–7]. Copot et al. [8] presented a fractional-order PKPD model for propofol diffusion and showed fitting via data. Toledo-Hernandez et al. [7] described the phenomenon associated with parameter fitting to the anomalous data of tequila using the fermentation process. Dokoumetzidis et al. [6] reported that some fractional-order models [9] are not consistent systems of equations, and discussed how to satisfy the law of conservation of mass [10]. Then, multi-compartment systems [5, 11] were introduced in order to explain drug absorption and the disposition process to solve the consistent problem.

Despite the presence of many studies that are related to FDEs [7, 8, 10, 12], which partially describe the PKPD phenomena in terms of the drug disposition and the drug effect, to the best of our knowledge, there are no models

that consider the fractional-order tumor growth inhibition (FTGI). In this work, we obtain the drug concentration using a drug disposition model, derive the appropriate effect function, and construct the FTGI model. We investigated the tumor decline phenomenon that elapsed after sufficient time had elapsed, and which could not be explained in the ODE model. In addition, the TGI system of ODEs requires unknown additional compartments to express the memory effect using linear tricks [13, 14], but not in the FTGI model. The differences in the equilibrium points and maximum tumor size between the FTGI and the ODE model with logistic growth and a number of inflection points that are dependent on the fractional order will be investigated.

We introduce a fractional drug disposition model, derive an Emax model mathematically, and substitute it into the FTGI model using Caputo derivative. Simulation results of the difference between the fractional order and the maximum tumor size are then explored. In addition, a suitable range of the fractional order should be chosen according to the concavity. Finally, we discuss the FTGI model.

A drug disposition model with a fractional-order derivative

We start with well-known drug disposition models [1, 8] as follows.

$$\begin{cases} \frac{dq_1}{dt} = -(k_{01} + k_{12} + k_{1e})q_1 + k_{21}q_2 \\ \frac{dq_2}{dt} = k_{12}q_1 - (k_{02} + k_{21})q_2 \\ \frac{dq_e}{dt} = k_{1e}q_1 - k_{0e}q_e, \end{cases}$$

where V_i , $i = 1, 2, e$, is the volume in i compartment and cl_i , $i = 1, 2, e$, is the clearance in i compartment, and

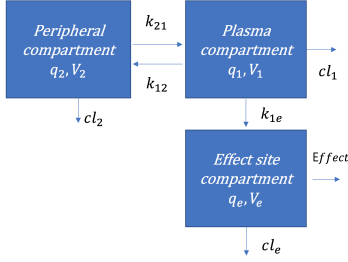


FIGURE 1. Drug disposition model

q_i , $i = 1, 2, e$, denotes the amount of a drug in i compartment. $C_1(t) = q_1/V_1$ is drug concentration in central compartment at t with unit nM , $C_2(t) = q_2/V_2$ is concentration in peripheral compartment at t , $C_e(t) = q_e/V_e$ is concentration in effect compartment at t . Constant rates k_{12} and k_{21} are inter-compartment rate constant with unit rate $time^{-1}$ and $k_{01} = cl_1/V_1$, $k_{02} = cl_2/V_2$ and $k_{0e} = cl_e/V_e$ are elimination rate constant with unit rate $time^{-1}$. k_{1e} is transfer rate constant for representing delay with unit rate $time^{-1}$. Thus,

$$\begin{cases} \frac{dC_1}{dt} = -(k_{01} + k_{12} + k_{1e})C_1 + k_{21}C_2, \\ \frac{dC_2}{dt} = k_{12}C_1 - (k_{02} + k_{21})C_2, \\ \frac{dC_e}{dt} = k_{1e}C_1 - k_{0e}C_e. \end{cases} \quad (1)$$

If we do not consider effect compartment and

consider mass transfer integrals containing a specific kernel to represent a memory effect: $G_{12}(t, \tau)$, $G_{21}(t, \tau)$, $G_{10}(t, \tau)$, and $G_{20}(t, \tau)$. Assuming that

$$G_{ij}(t, \tau) = \frac{(t-\tau)^{\alpha_{ij}-1}}{\Gamma(\alpha_{ij})}, \quad i = 1, 2, \\ j = 0, 1, 2, \quad 0 < \alpha_{ij} \leq 1.$$

Taking the first derivative of the above equations we end up with FDEs with

Riemann-Liouville

$$\frac{dC_1(t)}{dt} = -k_{01} \cdot {}_0D_t^{1-\alpha_{10}}C_1(t) - k_{12} \cdot {}_0D_t^{1-\alpha_{12}}C_1(t) + k_{21} \cdot {}_0D_t^{1-\alpha_{21}}C_2(t),$$

$$\frac{dC_2(t)}{dt} = k_{12} \cdot {}_0D_t^{1-\alpha_{12}}C_1(t) - k_{02} \cdot {}_0D_t^{1-\alpha_{20}}C_2(t) - k_{21} \cdot {}_0D_t^{1-\alpha_{21}}C_2(t).$$

Since RL is not practical due to fractional initial values, we should change them into Caputo derivative that appears with the following expression [15].

$${}_0D_t^{1-\alpha}f(t) = D^{1-\alpha}f(t) + \frac{f(0)t^{\alpha-1}}{\Gamma(\alpha)}.$$

The fractional drug disposition model from Eq.(1) with the initial value $C_1(0) = C_0(> 0)$ and $C_2(0) = 0$ are given by

$$\begin{cases} \frac{dC_1(t)}{dt} = -k_{01}D^{1-\alpha_{10}}C_1(t) - k_{12} \cdot D^{1-\alpha_{12}}C_1(t) + k_{21}D^{1-\alpha_{21}}C_2(t) - \\ k_{01} \frac{C_0t^{(\alpha_{10}-1)}}{\Gamma(\alpha_{10})} - k_{12} \frac{C_0t^{(\alpha_{12}-1)}}{\Gamma(\alpha_{12})}, \\ \frac{dC_2(t)}{dt} = k_{12}D^{1-\alpha_{12}}C_1(t) - k_{02} \cdot D^{1-\alpha_{20}}C_2(t) - k_{21}D^{1-\alpha_{21}}C_2(t) + \\ k_{12} \frac{C_0t^{(\alpha_{12}-1)}}{\Gamma(\alpha_{12})}, \end{cases} \quad (2)$$

where unit of the k_{ij} rate constants are $time^{\alpha_{ij}}$.

Emax and fractional-order TGI model

An Emax function, $E(t)$, is a description of drug effect over concentration [16]. $E(t)$ explains a dose-response curve governing binding of drug to an antigen by the law of mass action. Biological drug response reaches a maximum E_{max} similar to Michaelis-Menten equation[17]. The Emax model for inhibition by drug[18, 19] is usually given by

$$E(t) = \eta \left(E_0 - \frac{E_{max}c^\gamma}{IC_{50}^\gamma + c^\gamma} \right),$$

where E_0 is base drug concentration, E_{max} is maximum effect, IC_{50} is a concentration when the effect of the concentration reaches $E_{max}/2$, η is a positive constant, and Hill coefficient γ is a cooperative coefficient or sigmoid coefficient.

Assume that the tumor growth without injecting a drug is a logistic, and consider how the tumor volume is reduced by the effect function $E(t)$ using the linear death (elimination) rate (q_2). We first present well known TGI models [20]. Particularly, logistic growth ($1 - T/T_{max}$) [21] is used instead of exponential growth in [20] to consider finite equilibrium in a long time.

$$\frac{dT}{dt} = q_1 ET \left(1 - \frac{T}{T_{max}}\right) - q_2 T, \quad (3)$$

or

$$\begin{cases} \frac{dT}{dt} = kT \left(1 - \frac{T}{T_{max}}\right) - M_n T \\ \frac{dM_1}{dt} = \frac{1}{\tau_1} (E - M_1) \\ \frac{dM_i}{dt} = \frac{1}{\tau_i} (M_{i-1} - M_i), \end{cases} \quad (4)$$

where T is a tumor size with unit mm^3 , T_{max} is a maximum tumor size, M_1 is an elimination constant with unit $time^{-1}$, M_i is compartment for delay, and τ_i are average resident time constant with unit $time$, $\tau_i \in \mathbb{R}^+$, $i = 2, 3, \dots, n$. Eq.(4) is considered from a delay differential equation (DDE) to system of ODE by a linear trick in removal process [4, 14]. Contrary to above the TGI model, the FTGI model using fractional-order derivative based on [22] with Emax model is constructed as follows.

$$D^\alpha T = q_1 ET \left(1 - \frac{T}{T_{max}}\right) - q_2 T, \quad (5)$$

where T_0 is initial tumor size, $0 < \alpha \leq 1$ is a fractional-order, q_1 has $time^{-\alpha}$ constant, and a constant q_2 has a unit $time^{-\alpha}$.

Results

Laplace transform is applied to extract drug concentration from the fractional drug-disposition model. From Eq.(2), the following equation is expressed by taking Laplace transformation both sides:

$$\begin{cases} sY_1(s) - C_0 = -k_{01}(s^{(1-\alpha_{10})}Y_1(s) - s^{-\alpha_{10}}C_0) - k_{12}(s^{(1-\alpha_{12})}Y_1(s) - s^{-\alpha_{12}}C_0) + k_{21}s^{(1-\alpha_{21})}Y_2(s) - \left(\frac{k_{01}C_0}{s^{\alpha_{10}}} + \frac{k_{12}C_0}{s^{\alpha_{12}}}\right) \\ sY_2(s) = k_{12}(s^{(1-\alpha_{12})}Y_1(s) - s^{-\alpha_{12}}C_0) - k_{02}s^{(1-\alpha_{20})}Y_2(s) - k_{21}s^{(1-\alpha_{21})}Y_2(s) + \frac{k_{12}C_0}{s^{\alpha_{12}}}, \end{cases},$$

where

$$\mathcal{L}\left(t^{(\alpha_{ij}-1)}\right) = \frac{\Gamma(\alpha_{ij})}{s^{\alpha_{ij}}}, \quad 0 < \alpha_{ij} \leq 1.$$

Thus, Y_1 and Y_2 are given by

$$\begin{cases} Y_1(s) = \frac{(s+f_{20}+f_{21})C_0}{(s+f_{10}+f_{12})(s+f_{20}+f_{21})-f_{12}f_{21}} \\ Y_2(s) = \frac{f_{12}}{s+f_{20}+f_{21}}Y_1(s), \end{cases} \quad (6)$$

where $f_{ij}(s) = k_{ij}s^{1-\alpha_{ij}}$, $i \neq j$, $i = 1, 2$, and $j = 0, 1, 2$. We compare Eq.(3) and Eq.(5) by setting the value of α_{ij} to be “1” in order to determine whether the drug disposition model in Eq.(5) agrees with Eq.(3). In the case, there is no difference between the two models shown in Fig.2. The drug disposition, Emax model, and the TGI effect are investigated by solving (5) and (6).

The FTGI model is compared when the value of α is “1”, as shown in Fig.3. Various dynamics of FTGI are explored according to the α value. Obviously, it

TABLE 1. The parameter values, units, and explanations.

Parameter	Value	Unit
k_{01}	0.5	$time^{-10}$
k_{12}	0.5	$time^{-12}$
k_{02}	0.5	$time^{-20}$
k_{21}	0.5	$time^{-21}$
q_1	0.03	$time^{-\alpha}$
q_2	0.1	$time^{-\alpha}$
T_0	100	mm^3
E_{max}	20	unitless
IC_{50}	80	nM
E_0	50	nM
C_0	200	nM
T_{max}	5000	mm^3
α_{10}	(0, 1]	unitless
α_{12}	(0, 1]	unitless
α_{20}	(0, 1]	unitless
α_{21}	(0, 1]	unitless
α	(0, 1]	unitless

is clear that the larger the value of α , the more similar it is to the model (3).

Fig.2(a) shows various drug dynamics using values of α_{ij} that are generated by 1000 random numbers. A fast decline in the initial time phase is seen when α_{ij} is smaller. Contrary to the yellow curve, which represents (3), where the drug converges to zero with time, there is drug trapping as the value of α_{ij} becomes less than one. In Fig.2(b), we plot the largest (the orange curve that has the plus shape) and the smallest (the blue curve that has the star shape) values that were obtained by the mean square of the difference of the drug concentrations of Eqs.(5) and (3). The blue curve that has the star shape appears to have no difference from the orange curve that has the plus shape in the linear scale,

but in (c), it has a different shape in the log-scale. This is because of the power-law function owing to the values of α_{ij} . There are no curves below the yellow curve Eq.(3) except for a short initial period. From this, the fractional-order in the model indicates a drug-trapping effect. This is one reason for which Eq.(5) should be considered as a model to fit data for drug accumulation. By assuming a subitable fractional-order, it may be possible to obtain better PK simulation results for drug accumulation. Fig.3(a) implies the TGI effect, which is obtained by taking the drug concentration from (3) and (5) when $\alpha = 1$, and which shows no difference between (3) and (5) when $\alpha = 1$. Fig.3(b) are plotted the dynamics when different values of α are changed by 1000 iterations randomly. The larger the value of α , the greater is the delay that is observed in the initial phase. Interestingly, small values of α imply small tumor delay in the initial phase, but have small equilibrium values. Tumor growth (blue) based on (3) in Fig.3(a) is increased by the equilibrium point. The tumor growth based on (5) shows interesting dynamics. i.e., less delay in the initial phase and small equilibrium as α is smaller. This indicates that FTGI explains the abnormal kinetics of a drug that accumulates in the body and this enables decisions regarding flexible tumor-equilibrium points by a drug, unlike (3). More precisely, the TGI model based on (3) does not consider the long-time dynamics because the equilibrium point always reaches a constant number when T_{max} is constant, but in FTGI, flexible decisions about the tumor equilibrium by a drug administration are possible. Although

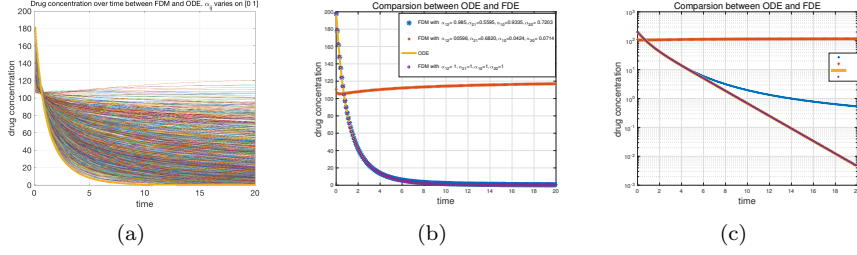


FIGURE 2. (a) Eq.(3) is plotted by the yellow curve, and various other curves are obtained using (5) with various values of α_{ij} . (b) The largest and smallest curves obtained the difference between (3) and (5) are plotted from (a). (c) Unlike the linear scale, the log scale shows that drug concentrations are different even though they appears to be similar in (b).

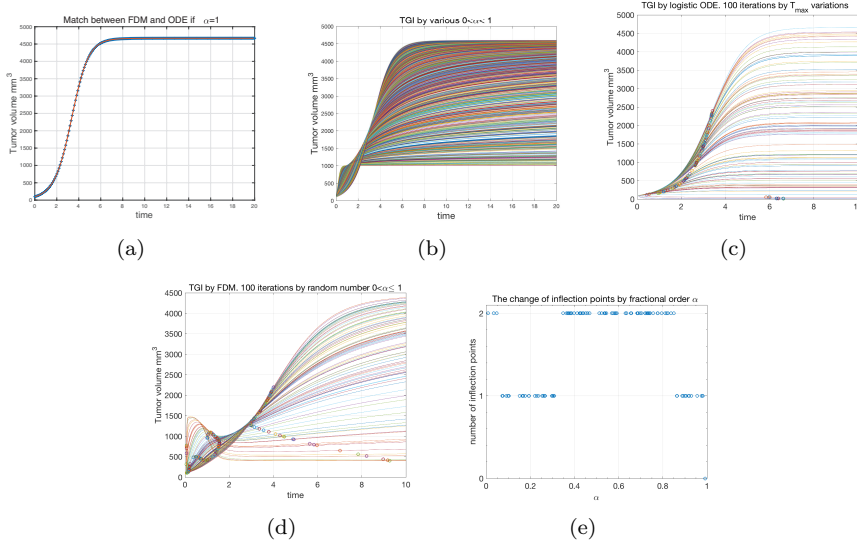


FIGURE 3. (a) There is no difference in the tumor sizes between FDE (5) and ODE (3) when $\alpha = 1$. (b) Curves are plotted with various values of $0 \leq \alpha \leq 1$. (c) A variation of the value of T_{max} in (3) and concavities. (d) Variation of α in (5) and concavities. (e) The number of concavities are different according to α .

the system based on ODEs has shown that the tumor is suppressed in the initial phase, and it eventually reaches the maximum value of the model when

the drug administration is stopped, the FTGI model supplies that the therapeutic effect can be observed with time

without the change of T_{max} . The difference between α in (5) and T_{max} in (3) are plotted. The number of concavities of (3) does not change, as shown in Fig.3(c); however, (5) does not, as shown in Fig.3(d). Figs. 3(c), (d), and (e) explain the concavity changes obtained using α on (5) and T_{max} on (3). The results generated by 100 iterations are plotted, and the time scale is limited by 10 days for a clear explanation. Inflection points in (3) follow a quadratic function up to the maximum tumor size of T_{max} , as shown in Fig.3(c), but the change in the inflection points according to α does not follow exponential, rational, or polynomial functions, as shown in Fig.3(d). Furthermore, the number of concavities is different from α . As seen in Fig.3(e), the number of inflection points over α is followed as the sum of step functions depends on α . This causes the number of inflection points on the FTGI model to not be fixed, and the shape does not increase nor decrease, unlike (3), as seen in Fig.3(c). Therefore, it is important to know the number of concavities from data to determine a suitable α .

Discussion

We have constructed the fractional-order model that can be used in drug-disposition and TGI. The FTGI model may describe an abnormal behavior of TGI data and present a criterion on how to determine a suitable fractional-order. The difference in tumor reduction are explored caused by fractional-order α and maximum tumor size T_{max} . The question that arises aims to determine the fast decline in the initial

phase and drug-trapping at the long time in the drug-disposition by α_{ij} . A possible reason is that the fractional order explains the accumulation effect of the drug. Dokoumetzidis et al. [10] explains that the fractional profile appears to be initially faster, but it eventually becomes slower. The slower kinetics arises as a result of the power-law kinetic of the terminal phase of the fractional case. The FTGI model indicates that the stronger tumor inhibition could be happened due to abnormal drug accumulation. As assuming a suitable fractional-order in vivo, the developed model may realize better simulation results when the drug disposition profile seems non-exponential terminal phases, the presence of which has been extensively acknowledged in the pharmaceutical literature, and with several approximation techniques, which should be proposed for fractional systems with different levels of accuracy, as explained in [23]. One of the next studies will discuss how to describe unusual tumor growth and inhibition with observable data. From (5), the fractional order remains the left side of the equation, but the reason remains unknown. Therefore, when a fractional order is attached to the right side of the equation, it should be investigated, and the reason should be clarified. Thus, in future study, we should explore the answer to this problem by studying different fractional-order models with physical meanings, and not ad-hoc models, but age-structure models using the stochastic process.

References

- [1] P. Macheras and A. Iliadis. *Modeling in Biopharmaceutics, Pharmacokinetics and Pharmacodynamics: Homogeneous and Heterogeneous Approaches*. Interdisciplinary Applied Mathematics. Springer International Publishing, 2016.
- [2] Bruce J. West and William Deering. Fractal physiology for physicists: Lvy statistics. *Physics Reports*, 246(1):1–100, 1994.
- [3] Christopher N Angstmann, Austen M Erickson, Bruce I Henry, Anna V McGann, John M Murray, and James A Nichols. Fractional order compartment models. *SIAM Journal on Applied Mathematics*, 77(2):430–446, 2017.
- [4] John E. Mittler, Bernhard Sulzer, Avidan U. Neumann, and Alan S. Perelson. Influence of delayed viral production on viral dynamics in HIV-1 infected patients. *Mathematical Biosciences*, 152(2):143–163, 1998.
- [5] Davide Verotta. Fractional dynamics pharmacokinetics–pharmacodynamic models. *Journal of Pharmacokinetics and Pharmacodynamics*, 37(3):257–276, Jun 2010.
- [6] Aristides Dokoumetzidis, Richard Magin, and Panos Macheras. A commentary on fractionalization of multi-compartmental models. *Journal of Pharmacokinetics and Pharmacodynamics*, 37(2):203–207, Apr 2010.
- [7] Rasiel Toledo-Hernandez, Vicente Rico-Ramirez, Gustavo A. Iglesias-Silva, and Urmila M. Diwekar. A fractional calculus approach to the dynamic optimization of biological reactive systems. Part I: Fractional models for biological reactions. *Chemical Engineering Science*, 117:217–228, 2014.
- [8] Dana Copot, Amelie Chevalier, Clara M Ionescu, and Robain De Keyser. A two-compartment fractional derivative model for propofol diffusion in anesthesia. In *Control Applications (CCA), 2013 IEEE International Conference on*, pages 264–269. IEEE, 2013.
- [9] Jovan K. Popovi, Milica T. Atanackovi, Ana S. Pilipovi, Milan R. Rapai, Teodor M, Stevan Pilipovi, and Atanackovi. A new approach to the compartmental analysis in pharmacokinetics: fractional time evolution of diclofenac. *Journal of Pharmacokinetics and Pharmacodynamics*, 37(2):119–134, Apr 2010.
- [10] Aristides Dokoumetzidis, Richard Magin, and Panos Macheras. Fractional kinetics in multi-compartmental systems. *Journal of Pharmacokinetics and Pharmacodynamics*, 37(5):507–524, 2010.
- [11] Jovan K. Popovi, Stevan Pilipovi, and Teodor M. Atanackovi. Two compartmental fractional derivative model with fractional derivatives of different order. *Communications in Nonlinear Science and Numerical Simulation*, 18(9):2507–2514, 2013.
- [12] Aristides Dokoumetzidis and Panos Macheras. Fractional

- kinetics in drug absorption and disposition processes. *Journal of Pharmacokinetics and Pharmacodynamics*, 36(2):165–178, 2009.
- [13] Prasith Baccam, Catherine Beauchemin, Catherine A Macken, Frederick G Hayden, and Alan S Perelson. Kinetics of influenza A virus infection in humans. *Journal of Virology*, 80(15):7590–7599, 2006.
- [14] Yusuke Kakizoe, Shinji Nakaoka, Catherine AA Beauchemin, Satoru Morita, Hiromi Mori, Tatsuhiko Igarashi, Kazuyuki Aihara, Tomoyuki Miura, and Shingo Iwami. A method to determine the duration of the eclipse phase for in vitro infection with a highly pathogenic SHIV strain. *Scientific Reports*, 5:10371, 2015.
- [15] Stefan G Samko, Anatoly A Kilbas, Oleg I Marichev, et al. Fractional integrals and derivatives. *Theory and Applications, Gordon and Breach, Yverdon*, 1993:44, 1993.
- [16] B Meibohm and H Derendorf. Basic concepts of pharmacokinetic pharmacodynamic (PK/PD) modelling. *International journal of clinical pharmacology and therapeutics*, 35(10):401–413, 1997.
- [17] Kenneth A. Johnson and Roger S. Goody. The Original Michaelis Constant: Translation of the 1913 MichaelisMenten Paper. *Biochemistry*, 50(39):8264–8269, 2011.
- [18] Meindert Danhof, Elizabeth CM de Lange, Oscar E Della Pasqua, Bart A Ploeger, and Rob A Voskuyl. Mechanism-based pharmacokinetic-pharmacodynamic (PK-PD) modeling in translational drug research. *Trends in Pharmacological Sciences*, 29(4):186–191, 2008.
- [19] Donald E Mager, Elzbieta Wyska, and William J Jusko. Diversity of mechanism-based pharmacodynamic models. *Drug Metabolism and Disposition*, 31(5):510–518, 2003.
- [20] Shinji Yamazaki, Judith Skaptason, David Romero, Joseph H. Lee, Helen Y. Zou, James G. Christensen, Jeffrey R. Koup, Bill J. Smith, and Tatiana Koudriakova. Pharmacokinetic-Pharmacodynamic Modeling of Biomarker Response and Tumor Growth Inhibition to an Orally Available cMet Kinase Inhibitor in Human Tumor Xenograft Mouse Models. *Drug Metabolism and Disposition*, 36(7):1267–1274, 2008.
- [21] Vinay G. Vaidya and Frank J. Alexandro. Evaluation of some mathematical models for tumor growth. *International Journal of Bio-Medical Computing*, 13(1):19–35, 1982.
- [22] Malgorzata Turalska and Bruce J. West. A search for a spectral technique to solve nonlinear fractional differential equations. *Chaos, Solitons & Fractals*, 102:387–395, 2017.
- [23] Pantelis Sopasakis, Haralambos Sarimveis, Panos Macheras, and

Aristides Dokoumetzidis. Fractional calculus in pharmacokinetics. *Journal of Pharmacokinetics and Pharmacodynamics*, 45(1):107–125, Feb 2018.

JONG HYUK BYUN

DEPARTMENT OF MATHEMATICS, PUSAN NATIONAL UNIVERSITY, GEUMJEONG-GU, BUSAN 46241, REPUBLIC OF KOREA

E-mail address: `maticax@gmail.com`

IL HYO JUNG

DEPARTMENT OF MATHEMATICS, PUSAN NATIONAL UNIVERSITY, GEUMJEONG-GU, BUSAN 46241, REPUBLIC OF KOREA

E-mail address: `ilhjung@pusan.ac.kr`